Korean J. Chem. Eng., 32(10), 2116-2123 (2015)
DOI: 10.1007/s11814-015-0051-9

pISSN: 0256-1115
eISSN: 1975-7220

Enhanced copper(II) biosorption on SiO_2-alginate gel composite: A mechanistic study with surface characterization

Sibel Yalçın*,†, Reşat Apak*, and İsmail Boz**

*Chemistry Department, Faculty of Engineering, Istanbul University, Avcilar 34320, Istanbul, Turkey
**Chemical Engineering Department, Faculty of Engineering, Istanbul University, Avcilar 34320, Istanbul, Turkey
(*Received 24 August 2014 • accepted 10 March 2015*)

Abstract−A new SiO_2-alginate biocomposite was synthesized with improved mechanical properties, showing chelation capability of divalent metal ions, especially Cu(II), through its carboxylic acid ends. The biocomposite was characterized using scanning electron microscopy (SEM), Fourier-transform infrared (FTIR), and X-ray photoelectron spectroscopy (XPS) techniques. The adsorption of copper(II) onto both H- and Ca-forms of sorbent was investigated as a function of pH and contact time, and adsorption data were modeled with the aid of Langmuir and Freundlich isotherms. The release of Ca(II) ions accompanying copper(II) binding was evaluated by selective surface complexation concept involving ion-exchange. The IR spectra gave detailed information on complexation of carbonyl group with copper ions and on the relative contribution of SiO_2 involved in copper uptake. The adsorption edge of copper was within the pH range 4.0-5.5, and the sorbent capacity was determined as 1.85 and 1.10 $mmolg^{-1}$ for H- and Ca-forms, respectively.

Keywords: Alginate-SiO_2 Biocomposite, Cu(II) Adsorption, FTIR-XPS Analyses, Surface Characterization

INTRODUCTION

Over the last two decades, microorganisms, plants, animals, and related biopolymers, including amino acid peptides, proteins and polysaccharides, have attracted much attention in chemistry and materials science in regard to metal-binding ability. Alginic acid, extracted more specifically from brown seaweed but also from bacteria, is one of the most abundant polysaccharides that contains many of the carboxyl functions including β-D-mannuronic(M) and α-L-gluronic acid(G) groups, having the capability to form insoluble hydrogel bead with calcium and other divalent cations in aqueous solution to yield a three-dimensional network described as egg-box structure [1-3]. As a result of such a unique structural property enabling metal binding selectivity, alginate and modified alginate derivatives have been used extensively for heavy metal removal. The main purpose of producing such modified materials (composites) is to provide a synergic effect, combining the properties of each component in the mixture. Recently, various modified alginate gel-based adsorbents have been proposed for a large number of different applications, such as removal of toxic inorganics-organics, controlled release of drugs and cell grafting. For example, an alginate zeolitic bead adsorbent was used for removal of nitrates, sulfate and Zn(II) ions from aqueous solutions by Chmielewska et al. [4]. They reported that the zeolitic aluminosilicate structure contributes significantly to mechanical strength and rigidity of biopolymeric alginate. Similarly, an alginate based adsorbent was prepared using immobilized kaolin to investigate the removal efficiency of copper ions from aqueous solution [5]. Several studies in the literature have also reported on removal of copper ions using different types of carboxylate-containing natural sorbents such as seaweed, chitosan modified with succinic anhydride, and spent coffee ground [6-8].

In addition to studies on the functionalities of all the bio-based sorbents, some researchers examined the surface characteristics of biomaterials and metal ion-sorbent interactions using various spectroscopic techniques such as SEM, TEM, FT-IR and XPS. Tam et al. [9] used a combination of three surface sensitive techniques, attenuated total reflectance Fourier transform infrared spectroscopy (ATR-FTIR), X-ray photoelectron spectroscopy (XPS) and time-of-flight secondary ion mass spectrometry (ToF-SIMS), to characterize the surface and membrane of the alginate based microcapsules (APA). The two techniques, IR and XPS, were applied by Serra et al. [10] to determine the bonding configuration of bioactive silica based materials and to confirm the presence of nonbridging silicon-oxygen groups. Figueria et al. [11] used FTIR and XPS techniques to investigate the iron binding mechanism of dried algal biomass. On the other hand, although the superior characteristics of biopolymeric calcium alginate beads are known as gellation and metal chelation, they also have certain disadvantages such as softness and tendency of slight solubilization (uncontrollable degradation). Consequently, they can be easily damaged during biosorption experiments in batch processes. Therefore, in order to enhance the mechanical, chemical and thermal stability of the gel-bead, one of the most promising inorganic support materials, micro powder SiO_2, was preferably used as a strengthening agent in the present work. Hence, an alginate-silica based biosorbent for copper binding was developed by combining gelling, swelling and metal chelating properties of alginate with mechanical and physico-chemical stability of

†To whom correspondence should be addressed.
E-mail: sibelyal@istanbul.edu.tr

micro powder silica. This work is particularly focused on the investigation of copper adsorption due to the dose-dependent toxic potential of copper at excessive levels, which can cause deposition in the human brain, skin, liver, pancreas and myocardium resulting in "Wilson's disease" [6].

The main objective of this study is also to reveal the structural and physico-chemical characteristics of silica-added alginate biocomposite compared to those of the copper-loaded form by means of sensitive analytical techniques as SEM, FTIR and XPS. The use of XPS technique also enabled us to determine the valence of copper ions sorbed onto silica-alginate bead. In addition to detailed surface characterization, copper adsorption was also studied as a function of solution pH, contact time and initial metal concentration by considering the relationship between copper retention and calcium release under the concept of selective surface complexation extensively modeled by Chen et al. [12].

EXPERIMENTAL SECTION

1. Materials

Sodium alginate and microsized silica (SiO_2) particles (5-25 μm) with high purity grade were provided from Sigma-Aldrich. All other chemicals were supplied from Merck (Darmstadt, Germany). Stock solutions of Cu(II) and Ca(II) were prepared by dissolving the appropriate amounts of $Cu(NO_3)_2 \cdot 3H_2O$ in 0.1 M HNO_3 solution and of $CaCl_2 \cdot 2H_2O$ in distilled water, respectively. The concentration of each working metal ion solution before and after adsorption was measured by using a Varian SpectrAAFS-220 atomic absorption spectrophotometer with an air-acetylene flame for atomization. All pH measurements were conducted with a Metrohm Herisau E-512 pH meter equipped with a glass electrode. It was calibrated against buffer solutions pH 4.0 and 7.0 prior to use.

2. Biocomposite Beads Preparation

The preparation of biocomposite was carried out as follows:

First, the biocomposite gel solution was formed by adding 0.2 g SiO_2 powder into 1.5% (w/v) sodium alginate solution and stirred until a homogeneous mixture was obtained (4 h) [13]. Then, the mixture was transferred to a burette and added dropwise into a 500 mL solution of 0.1 M $CaCl_2$ under constant stirring, which instantly resulted in spherical insoluble gel beads of approximately 3.0-3.5 mm diameter [14,15]. The beads were left in the solution overnight to complete the stabilization/hardening process, washed thoroughly with distilled water to eliminate residual chloride ions, and then dried on filter paper at room temperature until reaching constant weight. To avoid unfavorably high viscosity effects caused by a concentrated solution containing ≥2.0 wt% of alginate, the amount of alginate was preferably chosen as 1.5% (w/v) to obtain a homogeneous mixture. On the other hand, micro powder SiO_2 content was particularly fixed at 0.2 g due to the excessive hardness effect of greater amounts of this additive material. To get H-form biocomposite, a known amount of dried biocomposites was protonated by soaking in 0.1 M HCl with shaking in a rotary shaker at 150 rpm for three hours. After the protonation process, the biocomposite beads were washed thoroughly with deionized water until pH 4.5 was obtained and then dried at room temperature. The gel beads dried once were repeatedly used both in H- and Ca-form. However, when wet beads obtained by the first gelation were converted into protonated form using 0.1 M HCl, some degradation of the beads occurred. Hence, all experiments were performed by using dried form biocomposite.

3. Characterization Techniques

The complementary analysis techniques, SEM, FTIR, and XPS, were used to obtain analytical information about surface morphology and chemical composition of the biocomposite as well as the metallic ion-bead interactions, both before and after copper binding. Scanning electron micrographs were performed after gold coating on a field-emission SEM (FEI-QUANTA FEG 450) by examining fractured cross-sections of the samples. The infrared spectra of the samples were analyzed in KBr tablets with the aid of a Mattson 1000 FT-IR spectrometer. X-ray photoelectron spectroscopy (XPS) measurements were conducted by using Thermo Scientific K-ALPHA surface analysis system with Al $K\alpha$ anode at a base pressure of 10^{-9} Torr. The instrument was calibrated against $Au4f_{7/2}$ peak binding energy of 150 eV. The spectra of elements were recorded over different energy ranges with the pass energy of 30 eV. The XPS results were evaluated in binding energy format and each spectrum was smoothed and deconvoluted using PeakFit software version v4.05.

4. Batch Adsorption Procedure

Adsorption of Cu(II) onto 0.05 g of SiO_2 added alginate beads (termed as biocomposite) was carried out in 250 mL conical flasks containing 50 mL solutions of varying initial metal concentrations (10-1,000 mg L^{-1}). The sorbent-metal ion mixture solutions were shaken at 150 rpm for different pH values (2.0-5.5) and contact times (30-480 min) in a temperature-controlled incubator at 25 °C. After equilibration of adsorption, the samples were filtered, and the filtrate was analyzed using flame-AAS. All experiments were carried out in duplicate with the average presented in the results. The amount of Cu(II) adsorbed was calculated using the following mass balance equation:

$$q_e=(C_i-C_e)V/W$$

where q_e is the amount of metal taken up by the biocomposite, V is the solution volume, W is the weight of biocomposite, and C_i and C_e are the initial and equilibrium metal concentrations, respectively. By following the adsorption process with 1.5 mol L^{-1} Cu(II) solution to investigate the reusability potential of biocomposite beads, eight consecutive adsorption-desorption cycles were conducted using 25 ml of 0.2 M HCl and HNO_3 solutions as eluent for 30 min contact-time. After each adsorption-desorption cycle, the sorbent was washed several times with distilled water to eliminate residual unbound metal ion and excess of acid for next usage. Because of elution with acid, the experiments were preferably carried out with H-form sorbent except for the first cycle (Ca-form), to take advantage of both process simplicity and higher metal uptake capacity, meaning that conversion of H-form to Ca-form was not applied to remaining tests.

RESULTS AND DISCUSSION

1. Scanning Electron Microscopy (SEM) Analysis

From SEM images presented in Fig. 1(c), (d), (e), (f), alginate with a characteristic layer morphology and siliceous large lumps

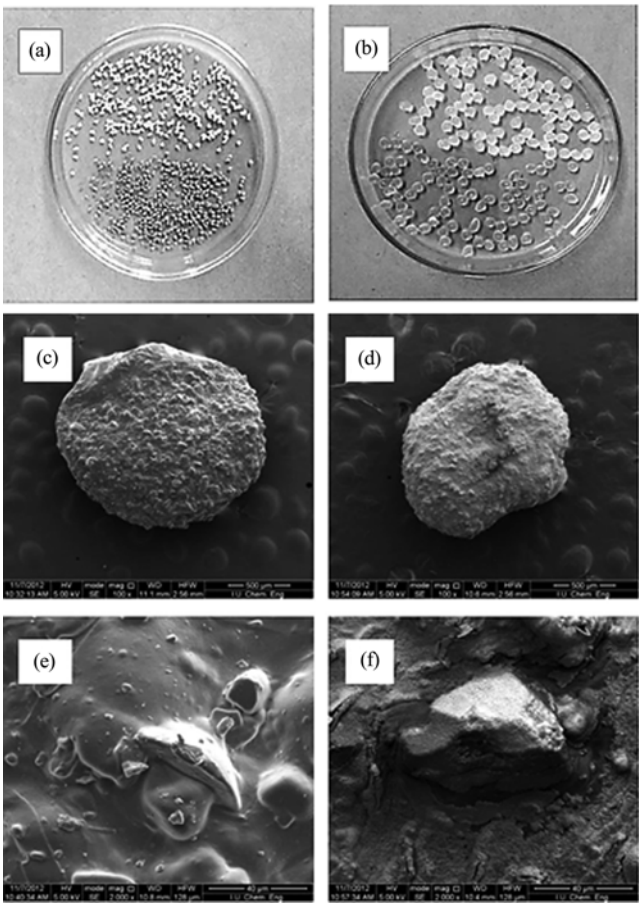

Fig. 1. Photographs ((a) (dried), (b) (wet)) and scanning electron micrographs of biocomposite beads before ((c) (×100), (e) (×2000)) and after ((d) (×100), (f) (×2000)) copper adsorption at different magnifications.

on the surface of pristine biocomposite beads was visualized, and after the saturation process, the presence of copper was clearly observed due to rough and rugged structure of the beads. Thus, the retention of copper was clearly demonstrated by photos of beads in dried and wet form, before and after copper loading (Fig. 1 (a-dried) and b-wet)).

2. Fourier-transform Infrared (FTIR) Analysis

FTIR analysis was performed with micro powder SiO_2, sodium alginate, SiO_2-alginate-Ca bead and copper loaded bead samples, presented in Fig. 2. The IR spectrum of silica exhibited a major characteristic band at about 1,095 cm^{-1} which was assigned to asymmetric stretching vibrations of Si-O-Si. The other characteristics absorption bands observed around 806 and 474 cm^{-1} were assigned to symmetric stretching (bending) vibration and out of plane (rocking) deformation of Si-O-Si chains in SiO_2, respectively. A weaker band at 1,620 cm^{-1} was attributed to O-H bending vibrations related to the hygroscopic nature of silica particles. The FTIR peak observed at 659 cm^{-1} was most probably indicative of a great density of Si-Si bonds which can be described as nonbridging hole center [16]. The peak at around 599 cm^{-1} could be related to Si-O stretching of the SiO_2 network defects [17].

Native alginate exhibited the main characteristic bands at 1,614 and 1,417 cm^{-1} corresponding to asymmetric and symmetric stretching peaks of carboxylate groups, respectively. The FTIR spectrum of the prepared SiO_2-alginate-Ca bead exhibited a series of new distinctive changes, which corroborates cross linking between alginate polymer and Ca ion in addition to specific peaks of powder SiO_2.

In the case of Cu loaded gel-bead of FTIR spectrum, the disappearance of the silica peaks between *ca.* 800 and 470 cm^{-1} showed that metal binding partially resulted from adsorption through the SiO_2 micro powder particles as well as from complexation with carboxylic groups of alginate. In addition, because of its more secondary nature of SiO_2 in comparison with alginate, the bands at around 1,030, 1,091 and 1,095 cm^{-1} from alginate and SiO_2 overlapped giving the single peaks at 1,100 and 1,078 cm^{-1} for calcium (cross-linked) and copper, respectively. The bands 1,032, 1,094 cm^{-1} were assigned to C-O stretching vibration of alcoholic hydroxyl groups of the natural saccharide (alginate) [18]. On the other hand, the overlapping of some peaks both in XPS and FTIR analysis was clearly caused by the presence SiO_2 in calcium alginate [5]. A decrease in intensity of the band at 1,100 cm^{-1} was observed and its location shifted significantly to 1,078 cm^{-1} after copper loading of biocomposite. The reduced and shifted peak at 1,078 cm^{-1} was assigned to alcoholic hydroxyl groups of alginate participating in copper binding, which is in line with the findings of XPS analysis [18,19]. In addition, the decrease and shift in position could also be explained by the relative contribution of SiO_2 in potential copper binding. As can be seen in Fig. 2, the intensity of bands at 1,614 and 1,417 cm^{-1} representing carboxylate groups considerably decreased and shifted from 1,614 to 1,628 cm^{-1} for copper, from 1,417 to 1,428 and 1,382 cm^{-1} for calcium and copper ions, respectively, which indicates complexation of the carbonyl group by dative coordination with metal ions [20-22]. In addition, the bands observed at 946, 888 and 820 cm^{-1} indicated the existence of guluronic and mannuronic acids, respectively [23] in alginate. Likewise, the observed peaks of guluronic and mannuronic acids mentioned above remarkably disappeared and shifted to lower frequency, which can be explained by the interaction of metal ion with the carboxylate groups. As a result, since alginate contains both polyhydroxy- and polycarboxylic acid groups, it plays a major role as a metal chelating agent [15,22].

3. X-ray Photoelectron Spectroscopy (XPS) Analysis

XPS analysis was applied to follow the changes in carbon 1s binding energy of the SiO_2 added Ca-alginate beads before (pristine) and after copper loading. We also examined O1s spectra of pristine and copper loaded biocomposite. Despite all our efforts, no meaningful interpretation was observed from the analysis of the O(1s) spectra after copper loading, due to the contribution of O(1s) emanating from SiO_2 in the structure. Hence, the data from (C1s) were interpreted carefully in line with the findings from FTIR analysis.

XPS spectra of pristine sample C(1s) was deconvoluted as the three types of carbon atoms attributed to C-C or C-H carbon at 285.08 eV, C-O-C (ether) or C-OH (alcoholic) carbon at 286.68 eV, and O=C-O (carboxylate) carbon at 288.58 eV. XPS spectra of copper loaded sample were also deconvoluted to the three types of carbon atoms observed in pristine one. The spectra of Cu loaded sample exhibited clear changes, which revealed copper binding [9]. As can be seen in Fig. 3(a), (b), the peak with binding energy of 288.58 eV,

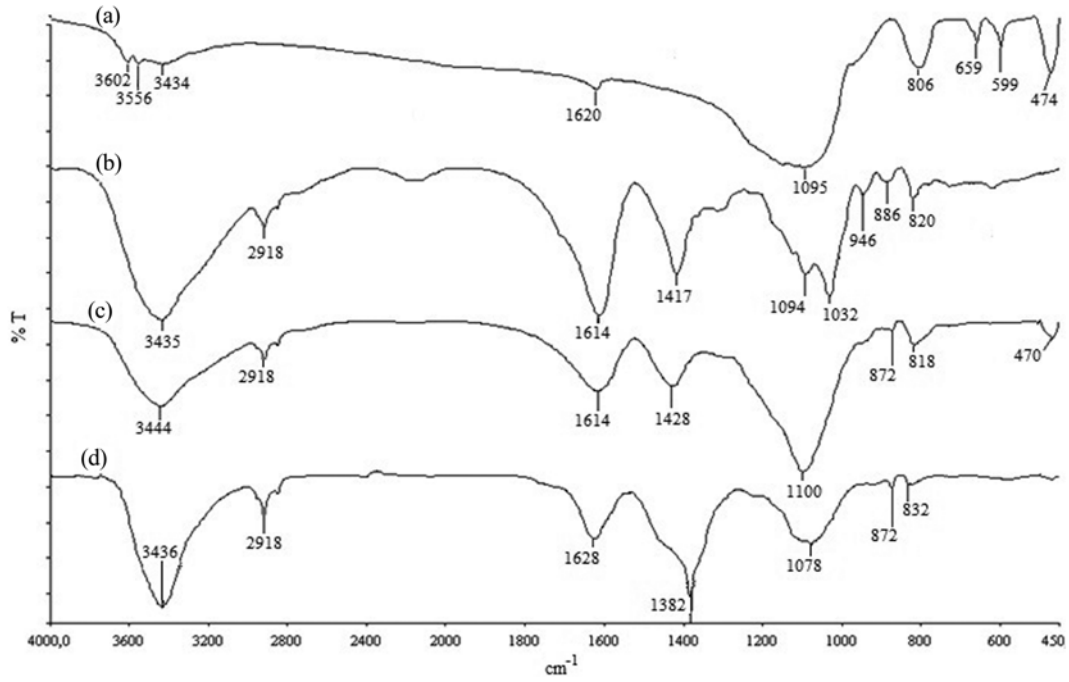

Fig. 2. FT-IR spectra of (a) SiO_2, (b) Sodium alginate, (c) SiO_2-alginate-Ca, (d) SiO_2-alginate-Cu.

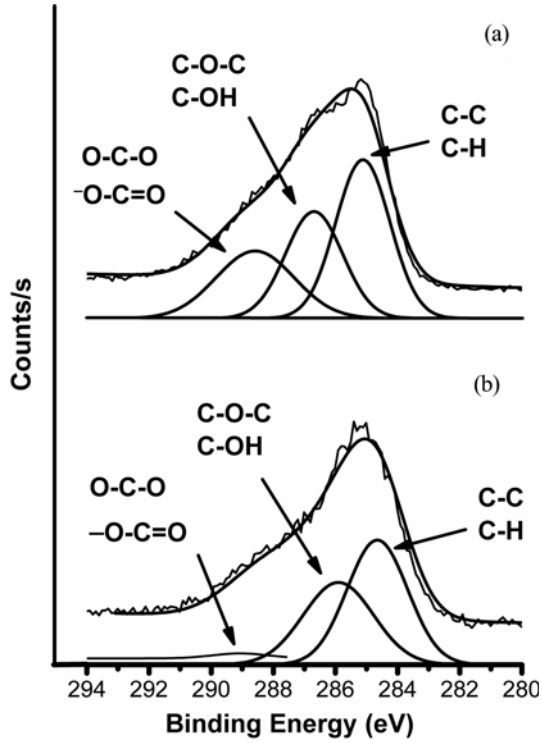

Fig. 3. XPS C1s spectra of SiO_2- alginate-Ca, ((a) pristine, (b) Cu-loaded).

which refers to carbon atom bonded to carbonyl and hydroxyl groups of the acid group, almost disappeared after copper loading [24]. This noticeable decrease indicated a change on the surface carboxylic acid groups of the sorbent caused by copper binding. Czanderna et al. reported a similar decrease of peak intensity in the surface acidic groups that was mainly derived from the interaction between copper and the single bonded oxygen portion of the acid group on the sorbent surface (corresponding to the unidentate -COOCu form of carboxylate species in our study) [24]. However, there is also a possibility of additional copper interaction with the C=O oxygen of the carboxylic acid groups as indicated in FTIR discussion. Carboxyl groups originating from guluronic and mannuronic acids of alginate were chiefly responsible for the ion exchange process and chelation with Cu^{2+} ions as in bidentate complexes, e.g., contributed by adjacent hydroxyl groups of the carboxylic and alcoholic functionalities on the surface, releasing two hydrogen ions per bound copper [19]. Hydroxyl groups were also present in alginate, but they presumably played a secondary role in copper binding [25].

On the other hand, decreases or disappearances of the peaks observed in XPS spectroscopy are frequently explained by the interaction of metal ion with the related surface functional groups of the sorbents. For instance, Chen et al. suggested that the decreases occurred in the peaks of alcoholic groups in XPS spectra of the Ca-alginate resin originating from Cu^{2+} adsorption through hydroxyl groups participating in coordination complex [26]. Likewise, Lim et al. reported a decrease in the peak of the single-bonded carbon oxygen C-O (alcoholic hydroxyl) after copper sorption [19]. In this study, a slight decrease in area of alcoholic groups and the slight shift of 0.8 eV suggest that alcoholic groups may have also participated in part to copper binding.

The Cu $2p_{3/2}$ spectra indicating the sorption of copper on the modified alginate are presented in Fig. 4. The spectra of Cu $2p_{3/2}$ photoelectrons were examined to verify functional groups containing oxygen and carbon involved in Cu^{2+} ion binding to SiO_2 added-alginate bead. Taking into account of the peak intensities of Cu^{2+} ions, it can be deduced that the first peak with binding energies of

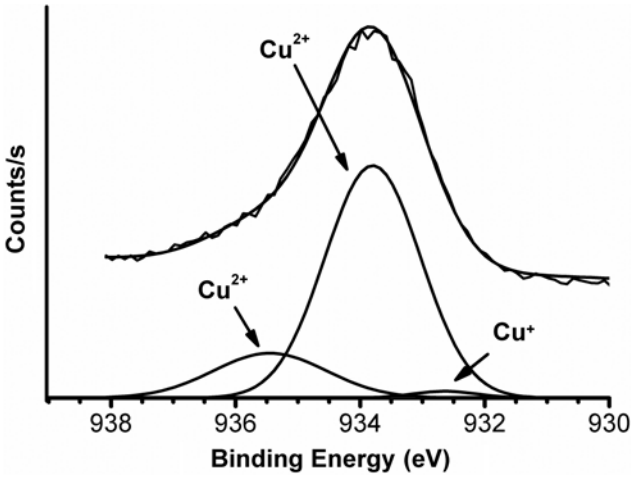

Fig. 4. XPS Cu2p spectra of copper-loaded biocomposite.

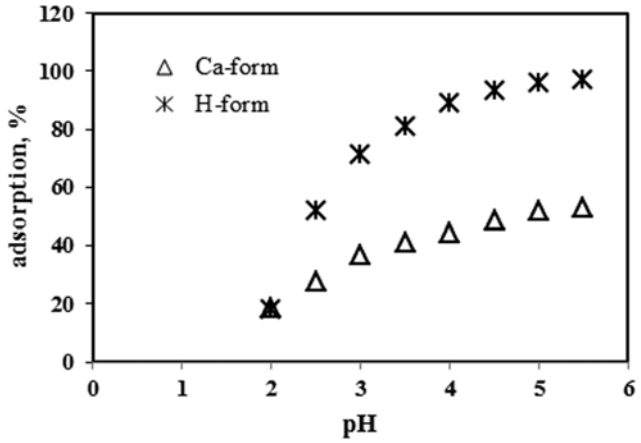

Fig. 6. Effect of pH on the biosorption of Cu(II) by SiO_2-alginate-Ca biocomposite (m_{beads}=0.05 g, initial copper concentration (C_o)=1.5 mmol L^{-1}, contact time=4 h).

933.78 eV has higher electron density of valence shell than the second peak with binding energies 935.48 eV [27]. The first peak at 933.78 eV was assigned to the alginate-bound Cu^{2+} as suggested by the literature reports [26,28]. The second peak at 935.48 eV represented Cu^{2+} located in the coordination sphere different from the prior one. We assign the peak at 933.78 eV to Cu^{2+} bound to alginate *via* unidentate carboxylate oxygen (-COOCu). In addition, it can be speculated that the peak at 935.48 eV could be due to the Cu^{2+} bound *via* hydroxyl groups and/or Cu^{2+} located in coordination sphere in line with Chen's comments [26]. Regarding the two different peak areas, the first type of coordination sphere is the more usual one compared to the second type, as can be seen in Fig. 4.

4. Effect of Contact Time on Adsorption

To investigate effective contact time for adsorption of Cu(II), experiments were conducted at different time intervals (30-480 min) and 150 rpm stirring speed for mixtures containing 1.5 mmol/L of 50 mL copper(II) solutions and 0.05 g biosorbent. As can be seen from Fig. 5, adsorption rate gradually increased up to 240 min and then practically reached a plateau with 53% adsorption; therefore, 240 min (4 h) was chosen as the appropriate batch-time for all the adsorption experiments. As Chen et al. have kinetically modeled the adsorption of copper(II) onto Ca-alginate as a combination of initially fast chemical reaction-controlled and slower intraparticle diffusion-controlled steps [12], this rather slow equilibration of copper sorption by alginate beads is understandable.

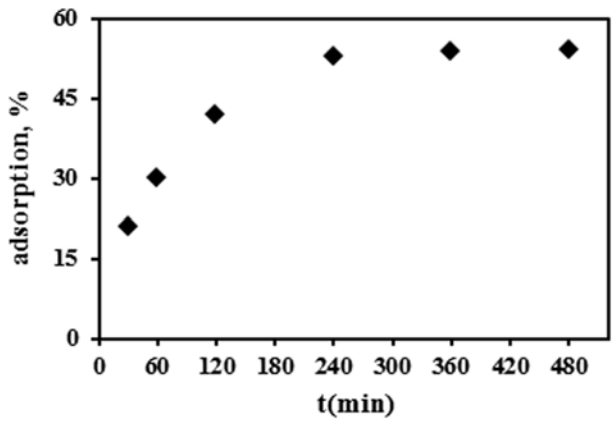

Fig. 5. Effect of contact time on the adsorption of Cu(II) by SiO_2-alginate-Ca biocomposite (pH_e=5.0, m_{beads}=0.05 g, initial copper concentration (C_o)=1.5 mmol L^{-1}).

5. Effect of Equilibrium pH on Adsorption

As presented in Fig. 6, the effect of pH on copper(II) adsorption by natural (SiO_2-alginate-Ca) and protonated sorbents was studied up to pH 5.5, thereby avoiding possible precipitation of metal ion that could have occurred at higher pH values. Starting from pH 2.0 where copper(II) showed the same weak retention percentage for both of the mentioned forms depending on the competitive effect of hydrogen ions, H-form exhibited a sharp increase in adsorption capacity with pH compared to the natural one (*i.e.*, Ca-form). Since the prepared SiO_2-alginate-Ca biocomposite (having a zig-zag structure) containing guluronic and mannuronic acid has chelating effect on metal binding, Cu more easily replaced H than Ca from H- and Ca-forms, respectively, during the binding process, because Ca(II) is a competitive metal cation in selective surface complexation. Also the guluronic acid residue in alginates has higher selectivity for Ca, which is a divalent cation compared to monovalent H and Na [29]. The carboxylic acid (*i.e.,* mannuronic (M) and guluronic (G) acids) residues in alginic acid have acidic dissociation constants as pK_a=3.38 and 3.65, respectively [30]. As can be seen from Fig. 6, the pH interval for increased copper sorption was between pH 3.5-5.0, in accordance with the related carboxylic acid pK_a values, because deprotonated carboxylate groups were more effective for Cu-chelation. In copper(II) sorption, the point of zero charge (pzc) of natural alginic acid reported as pH_{pzc}= 2.8 by Jeon et al. [31] should also be taken into account, as above this pH, cation adsorption is favored.

6. Relationship of Copper Retention with Calcium Release as a Function of Equilibrium pH

To reveal the pH-dependent nature of Ca(II) release from biomaterial accompanying Cu(II) uptake, experiments were performed with both deionized water (*i.e.*, copper-free medium) and copper containing solutions in the pH range of 2.0-5.5. In the presence of

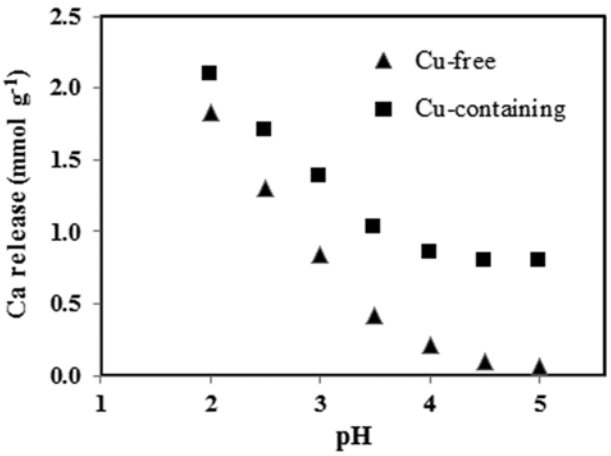

Fig. 7. Ca release of biocomposite beads to solution in Cu-free and Cu-containing media as a function of equilibrium pH (m_{beads} =0.05 g, initial copper concentration (C_o)=1.5 mmol L^{-1}).

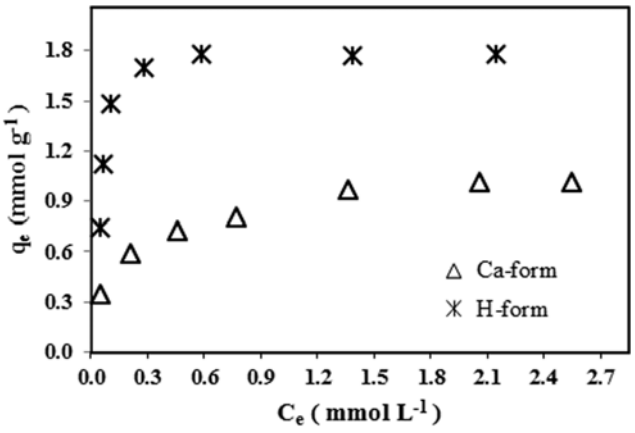

Fig. 8. Langmuir isotherms for the adsorption of Cu(II) onto H- and Ca-form biocomposite (50 mL solution contacted with 0.05 g biocomposite beads for 4 h, at 25 °C).

copper(II) ions, the quantity of Ca ions released from beads to solution gave the total number of Ca ions by the replacement of copper and protons. When working with copper-free solution, Ca-release was only dependent on pH changes, *i.e.*, Ca was released with increasing acidity. So, the portion of released Ca ions completely originating from copper binding was calculated by difference (Fig. 7). Since released calcium ions matched replaced copper ions at a stoichiometric mole ratio of 1 : 1 for the tested pH, copper sorption process can be partly explained with the aid of ion exchange mechanism. Although Chen et al. proposed a two-pK_a surface complexation model for Cu(II) uptake by Ca-alginate involving the simultaneous binding of SO^-Cu^{2+} and SO^-CuOH^+ complexes to the surface (SO^-) groups, they also considered the significant involvement of ion exchange mechanism in Cu(II) retention [12]. Due to the extremely weak competitive effect of hydrogen ions at pH 4-5 (Fig. 7), the release of Ca ions from the beads occurred at trace level for weakly acidic copper-free solutions. Thus, after contact with copper solution, the Ca(II) ions release into solution from the beads between pH 3-5 was almost entirely caused by the replacement of copper ions. For instance, on a molar basis, a copper retention of 0.82 mmol/g-biomaterial corresponded to a Ca(II) release of 0.74 mmol/g-biomaterial at pH_{eq}=5.0, verifying the ratio as $[Cu]_{ads.}/[Ca]_{rel.}$= 1.1±0.1.

7. Adsorption Equilibrium

The equilibrium adsorption data of Cu by both H- and Ca-forms of SiO_2 added alginate composites are presented in Fig. 8. As can be seen, the copper sorption rate as a function of copper concentration in solution was much steeper for H-form biocomposite than for Ca-form until saturation capacity was reached, which indicates the stronger affinity of H-form toward Cu(II) ions. This is most likely related to the effect of guluronic acid groups in alginate showing more selectivity of H-form sorbent toward copper than Ca-form biocomposite at constant pH=5.0 [29].

The experimental data were analyzed by Langmuir and Freundlich adsorption models [32], and the results fitted better to the Langmuir isotherm, suggesting that the surface of biocomposite beads for copper adsorption is homogeneous and limited to monolayer coverage.

The Langmuir equation can be written as follows:

$$q_e=q_m\, bC_e/(1+bC_e)$$

where q_m (mmol/g) is the monolayer adsorption capacity of the biocomposite, C_e is the equilibrium metal ion concentration in the solution (mmol L^{-1}) and b (L $mmol^{-1}$) is an affinity constant, respectively. The linearized Langmuir model can be formulated as:

$$C_e/q_e=C_e/q_m+1/(b\, q_m)$$

The linearized Freundlich model is

$$\text{Log } q_e=\text{Log } K_F+(1/n)\text{ Log } C_e$$

where K_F (L mol^{-1}) is a constant related to extent of metal ion removal and n is an empirical parameter related to biosorption intensity, which were calculated from the intercept and slope of the plot, respectively. In accordance with data processing with the aid of a linearized Langmuir isotherm equation, the saturation capacity q_m was found 1.85 and 1.10 $mmolg^{-1}$ for H-form and Ca-form biocomposite, respectively. Langmuir model fitted the experimental data better than the Freundlich model for Ca-form and particularly H-form biocomposite regarding the closeness of correlation coefficients (R^2) to 1.0. However, the values of n>1.0 from Freundlich model indicated that the adsorption of Cu(II) with both forms of biocomposite was favorable at studied conditions, as can be seen from Table 1.

While the Langmuir adsorption isotherm can be a useful approximation of most experimental data on heterogeneous surfaces where adsorption reaches saturation over a critical equilibrium concentration of the adsorbate in the aqueous phase, it does not fully explain what naturally happens in physical reality [33]. The deviation from the Langmuir isotherm arises from either the presence of multiple inequivalent sites with different binding energies on a given surface that can hold the adsorbate, or intermolecular adsorbate-adsorbate or adsorbate-solvent interactions.

As a result, it can be deduced that although monolayer adsorption onto uniform sites of a homogenous surface gives rise to a Langmuir equation, fitting of experimental data to a Langmuir model

Table 1. Langmuir and Freundlich isotherm parameters for copper adsorption onto SiO_2-alginate biocomposite

Sorbent	Langmuir constants			Freundlich constants		
	q_m (mmol g^{-1})	b (L $mmol^{-1}$)	R^2	K_F (L $mmol^{-1}$)	n	R^2
H-form	1.85	82.739	0.999	1.075	7.491	0.826
Ca-form	1.10	8.515	0.996	0.910	5.640	0.992

by itself does not necessarily imply that adsorption has actually occurred on monoenergetic sites with uniform binding energies for the adsorbate molecules. Likewise, the adjustable parameters in the two-surface Langmuir equation cannot be interpreted in terms of surface reactions without additional, independent evidence that only adsorption on two kinds of surface site actually is involved in the ion sorption reaction [34]. These discussions support the fact that fitting of our adsorption data to a Langmuir isotherm does not contradict the presence of different surface sites responsible for copper sorption.

The difference in the amount of Cu(II) adsorbed between H- and Ca-forms could be further explained by certain metal ion properties, such as ionic radii and electronegativity. This was also supported by Wase and Foster [35] that polysaccharides with carboxylate groups show preferential binding of cations with large ionic radii. This means that copper ions replaced hydrogen ions more easily than calcium ions from the surface of biocomposite beads, depending on equilibrium pH. Also among the divalent cations of first-row transition metals in the periodic table, copper(II) is the strongest complex-forming element regardless of the nature of ligand, also known as Irving-Williams order of complex formation.

8. Reusability

As seen in Table 2, the adsorption capacity of the sorbent increased significantly after the first cycle due to the higher copper binding tendency of H-form sorbent in preference over Ca-form, and additionally, the sorbent practically maintained both the same binding and reusability performance even after the 8^{th} cycle.

CONCLUSION

Sensitive analytical techniques, SEM, FTIR and XPS, were used to investigate structural and physico-chemical characteristics of silicium dioxide-added alginate biocomposite in comparison to those of copper-loaded form based on adsorption studies from aqueous solution. After copper binding, FTIR and XPS analyses revealed the changes corresponding to copper uptake essentially through carboxylic groups of alginate. Adsorption experiments were performed as a function of solution pH, contact time and equilibrium metal ion concentration, and the results were modeled with the aid of Langmuir and Freundlich isotherms. The Langmuir capacities of the biocomposite were found as 1.85 and 1.10 $mmolg^{-1}$ for H-form and Ca-form, respectively. The relationship of copper retention with concomitant calcium release as a function of equilibrium pH was evaluated by selective surface complexation and ion-exchange concepts. The molar ratio of retained Cu-to-released Ca was calculated as 1.1±0.1 at pH_{eq}=5.0. The potential advantages of the developed SiO_2-alginate composite sorbent in heavy metal removal from aqueous media were presented by its favorable properties of low-cost, excellent biocompatibility and biodegradability in addition to reusability.

Table 2. Reusability efficiency of SiO_2-alginate biocomposite

Cycle	Adsorption efficiency, %	Desorption efficiency, %	
		HCl	HNO_3
1	53	98,1	99.0
2	97	98.2	99.0
4	94	98.0	99.3
6	96	98.1	98.6
8	95	97.8	98.7

m_{beads}=0.05 g, initial copper concentration (C_o)=1.5 mmol L^{-1}

ACKNOWLEDGEMENTS

The authors gratefully acknowledge the research support provided by Istanbul University, Scientific Research Fund (Project grant No: UDP-34670 and BYP-32473/2013).

REFERENCES

1. M. R. Torres, A. P. A. Sousa, E. A. T. Silva Filho, D. F. Melo, J. P. A. Feitosa, R. C. M. de Paulab and M. G. S. Lima, *Carbohydr. Res.*, **342**(14), 2067 (2007).
2. T. A. Davis, B. Volesky and A. Mucci, *Water Res.*, **37**(18), 4311 (2003).
3. S. Yalcin, S. Sezer and R. Apak, *Environ. Sci. Pollut. Res.*, **19**(8), 3118 (2012).
4. E. Chmielewska, L. Sabova, H. Peterlik and A. Wu, *Braz. J. Chem. Eng.*, **28**(1), 63 (2011).
5. Y. Li, B. Xia, Q. Zhao, F. Liu, P. Zhang, Q. Du, D. Wang, D. Li, Z. Wang and Y. Xia, *J. Environ. Sci.*, **23**(3), 404 (2011).
6. V. Murphy, H. Hughes and P. McLoughlin, *Water Res.*, **41**(4), 731 (2007).
7. I. S. Lima and C. Airoldi, *Colloids Surf., A.*, **229**(1-3), 129 (2003).
8. N. E. Davila-Guzman, F. de J. Cerino-Cordova, E. Soto-Regalado, Soto-Regalado, J. R. Soto-Regalado, P. E. Diaz-Flores, M. T. Garza-Gonzalez and J. A. Loredo-Medrano, *Clean.*, **41**(6), 557 (2013).
9. S. K. Tam, J. Dusseault, S. Polizu, M. Menard, J.-P. Halle and L. H. Yahia, *Biomaterials*, **26**(34), 6950 (2005).
10. J. Serra, P. Gonzalez, S. Liste, C. Serra, S. Chiussi, B. Leon, M. Perez-Amor, H. O. Ylanen and M. Hupa, *J. Non-Cryst. Solids*, **332**(1-3), 20 (2003).
11. M. M. Figueira, B. Volesky and H. J. Mathieu, *Environ. Sci. Technol.*, **33**(11), 1840 (1999).
12. J. Chen, F. Tendeyong and S. Yiacoumi, *Environ. Sci. Technol.*, **31**(5),

1433 (1997).
13. F. Wang, J. Zhao, F. Pan, H. Zhou, X. Yang, W. Li and H. Liu, *Ind. Eng. Chem. Res.*, **52**(9), 3453 (2013).
14. J.-W. Choi, K.-S. Yang, D.-J. Kim and C. E. Lee, *Curr. Appl. Phys.*, **9**(3), 694 (2009).
15. H. G. Park, T. W. Kim, M. Y. Chae and I.-K. Yoo, *Process Biochem.*, **42**(10), 1371 (2007).
16. J. A. Luna-Lopez, J. Carrillo-Lopez, M. Aceves-Mijares, A. Morales-Sanchez and C. Falcony, *Superficies y Vacío*, **22**(1), 11 (2009).
17. R. Al-Oweini and H. El-Rassy, *J. Mol. Struct.*, **919**(1-3), 140 (2009).
18. E. Torres, Y. N. Mata, M. L. Blazquez, J. A. Munoz, F. Gonzales and A. Ballester, *Langmuir*, **21**(17), 7951 (2005).
19. S.-F. Lim, Y.-M. Zheng, S.-W. Zou and J. P. Chen, *Environ. Sci. Technol.*, **42**(7), 2551 (2008).
20. E. Fourest and B. Volesky, *Environ. Sci. Technol.*, **30**(1), 277 (1996).
21. S. Yalcin, *Clean.*, **42**(3), 251 (2014).
22. S. J. Kleinübing, R. S. Vieira, M. M. Beppu, E. Guibal and M. G. Carlos da Silva, *Mat. Res.*, **13**(4), 541 (2010).
23. E. Broderick, H. Lyons, T. Pembroke, H. Byrne, B. Murray and M. Hall, *J. Colloid Interface Sci.*, **298**(1), 154 (2006).
24. A. W. Czanderna, D. E. King and D. Spaulding, *J. Vac. Sci. Technol. A*, **9**(5), 2607 (1991).
25. S. K. Papageorgiou, F. K. Katsaros, E. P. Kouvelos, J. W. Nolan, H. Le Deit and N. K. Kanellopoulos, *J. Hazard. Mater.*, **137**(3), 1765 (2006).
26. J. P. Chen, L. Hong, S. Wu and L. Wang, *Langmuir*, **18**(24), 9413 (2002).
27. P. X. Sheng, Y.-P. Ting, J. P. Chen and L. Hong, *J. Colloid Interface Sci.*, **275**(1), 131 (2004).
28. X. Cheng, H. Guan and Y. Su, *J. Inorg. Organomet. Polym.*, **10**(3), 115 (2000).
29. M. M. Figueira, B. Volesky, V. S. T. Ciminelli and F. A. Roddick, *Water Res.*, **34**(1), 196 (2000).
30. A. Haug, *Acta. Chem. Scand.*, **15**(8), 1794 (1961).
31. C. Jeon, J. Y. Park and Y. J. Yoo, *Water Res.*, **36**(7), 1814 (2002).
32. S. Rengaraj, J.-W. Yeon, Y. Kim, Y. Jung, Y.-K. Ha and W.-H. Kim, *J. Hazard. Mater.*, **143**(1-2), 469 (2007).
33. R. I. Masel, *Principles of Adsorption and Reaction on Solid Surfaces*, Wiley-Interscience, New York (1996).
34. G. Sposito, *Soil Sci. Soc. Am. J.*, **46**(6), 1147 (1982).
35. J. Wase and C. F. Foster, *Biosorbents for Metal Ions*, Taylor & Francis Ltd., London, United Kingdom (1997).